Haline Convection in Polynyas and Leads

THEODORE D. FOSTER
Scripps Institution of Oceanography, La Jolla, Calif. 92037

(Manuscript received 16 May 1972, in revised form 15 June 1972)

ABSTRACT

A theoretical analysis of haline convection induced by the freezing of sea water is made for a turbulent ocean. The nonlinear equations for two-dimensional flow are solved using the mean field approximation and expanding the variables in Fourier series. It is found that, when the depth of the mixed layer is sufficiently large, the convective process is independent of depth. Expressions for the horizontal spacing of convection cells, maximum vertical velocity, and time required for manifest convection to develop are derived for a range of Schmidt numbers appropriate for the ocean. The analysis is applied to conditions that may be typical of freshly frozen polynyas or leads in the Weddell Sea, and it is concluded that haline convection is probably an effective process as a precursor to Antarctic Bottom Water formation.

1. Introduction

Though the formation of Antarctic Bottom Water is not yet completely understood, it is now widely believed from the work of Brennecke (1921) and Mosby (1934) that a primary influence upon the formation process is the increase in salinity of the surface waters brought about by the freezing of sea water. On the basis of water mass analysis Deacon (1937) and Wüst (1938) have shown that Antarctic Bottom Water is probably formed mainly in the Weddell Sea. The only data from the Weddell Sea for the southern winter were taken by the *Deutschland*. Fig. 1 shows the temperature and salinity profiles taken during the *Deutschland*'s drift across the Weddell Sea during the winter of 1912. The data are strongly influenced by the drift from about 73°50′S, 31°10′W where the ship froze in on 8 March to about 63°40′S, 35°50′W on 28 November when the ship became free. This can most clearly be seen in the temperature profiles where the transition from surface to intermediate water, commonly called the warm deep water, varies in depth and gradient in a non-monotonic way. The temperature of the surface water, however, did not vary much and remained quite close to the freezing point. The salinity of the surface water increased monotonically up to station 70, on 26 August, after which it started to decrease slowly. These data seem to support the idea that purely haline convection carries the brine excluded from the sea ice into the isothermal surface water layer.

In the shallow shelf regions of the southwest Weddell Sea this process can increase the salinity of the entire water column, while in the deeper regions the warm deep water evidently prevents the convection from penetrating very deeply, as suggested in Fig. 1. When the shelf water reaches a salinity of 34.51‰, it can mix with the adjacent warm deep water and form a mixture that is denser than the warm deep water. This process is known as cabbeling and evidently was first discussed by Witte (1902). The dynamics of cabbeling for two water types in juxtaposition have not been investigated so the effectiveness of the process cannot be accurately evaluated, but rough calculations seem to indicate that the process should be important at the shelf edge. In the deep regions of the Weddell Sea haline convection can again increase the salinity of the surface water to 34.51‰ providing a superposition of the two water types. In this arrangement cabbeling can cause an instability to develop since the mixture of the two water types is denser than the underlying warm deep water. Blobs of the dense mixture may then fall through the warm deep layer and produce bottom water (Foster, 1972). In either case haline convection seems to be a necessary precursor to Antarctic Bottom Water formation.

Badgley (1966) has pointed out that polynyas and leads may be very important to the heat budget of polar seas. This can be seen by considering the freezing of a sheet of ice. The heat flux through the ice sheet is given approximately by $k\Delta T/I$ where k is the average conductivity of the ice, ΔT the temperature difference across the ice sheet, and I the thickness of the ice. The heat flux is balanced by the latent heat given up by the water when it freezes at the bottom of the ice sheet, and is given by $\rho L\dot{I}$ where ρ is the density, L the latent heat of fusion, and $\dot{I}$ the rate of freezing of the ice sheet. Thus, the rate at which the ice freezes is approximately $k\Delta T/(\rho LI)$. We see from this that ice formation in a newly frozen lead or polynya with a 1 cm thick ice sheet will be two orders of magnitude faster than under sea ice 1 m thick. In the Arctic it has been estimated that the amount of open water is from less than 1% (Badgley, 1966) to more than 10% (Wittmann and Schule, 1966). What is needed is an estimate of not only the amount of open water but also the amounts of relatively thin ice where the heat transfer is also large. In the Antarctic even less is known about the ice cover in winter, and it may be quite different from the Arctic since ice is rapidly advected away from the continent to the north as evidence by the drifts of the *Deutschland* and *Endurance*. From an examination of satellite photographs Fletcher (1969) has surmised that large semi-permanent polynyas *may* exist near the Antarctic continent, in particular, in regions where the coastline trends NE-SW as in the southeastern Weddell Sea. Fig. 2 shows a photograph of a polynya near the Filchner Ice Shelf. Though this was summer, a cold strong katabatic wind with a temperature of about −20C and a speed of about 10 m sec^{-1} was blowing off the ice shelf. Around 8 cm of ice formed in 8 hr, which is in good agreement with the rate that would be estimated from heat flux considerations (like above). It should be noted that despite the relatively strong wind, the ice formed in very large, very flat sheets. Thus, it appears that the amount of salt introduced into the sea water by ice formation in leads and polynyas forms an important, if not dominant, part of the total salt flux into polar seas.

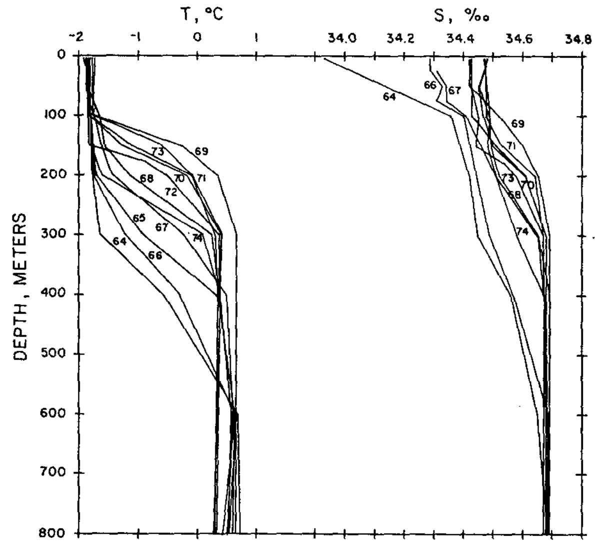

FIG. 1. Temperature and salinity profiles in the Weddell Sea taken while the *Deutschland* was frozen in and drifting with the ice pack from March to December, 1912; numerals indicate series number (data from Brennecke, 1921).

The analysis of haline convection under rapidly growing flat ice sheets in polynyas and leads crucially depends upon the horizontal scale of the convective flow. If the horizontal scale is large compared to the width of a typical lead, then the convection will be dominated by the horizontal inhomogeneity. This is the situation considered by Coachman (1966). On the other hand, if the horizontal scale is small compared

FIG. 2. *ARA General San Martin* in a large polynya just north of the Filchner Ice Shelf, February 1969. The ice is forming in large, flat sheets at an average rate of about 1 cm hr^{-1}. Wind was from the southeast at about 10 m sec^{-1}, air temperature about −20C.

to the width of the lead, then the convection will be dominated by a hydrodynamic instability mechanism. It will be shown later that the horizontal scale of the haline convection is indeed in most cases small compared to that of the width of most leads and polynyas, and thus the analysis for horizontally homogeneous conditions is appropriate.

Zubov (1943) has considered the mixing process induced by haline convection from the point of view of the static balance of layers. While this approach gives some idea of the extent that haline convection can penetrate in a stratified ocean it does not consider the time dependence or the dynamics of the process. Foster (1968a) has made a theoretical analysis of haline convection with a time-dependent approach. The prediction of cell spacing using this theory was verified by laboratory experiments (Foster, 1969). This analysis, however, used the linearized equations and thus cannot determine the velocities of the convection after onset. Another shortcoming of this theory is that, strictly speaking, it is only appropriate for molecular exchange coefficients since it uses an infinite Schmidt number. It is the purpose of the present paper to extend the theoretical analysis to include nonlinear effects so that velocities can be determined, and to consider a range of Schmidt numbers that are appropriate for the eddy exchange coefficients of a turbulent ocean. Then it will be possible to estimate the effectiveness of haline convection as a precursor to Antarctic Bottom Water formation.

2. Theoretical model

When sea water with a salinity $>24.7‰$ is cooled from above, thermal convection will produce a layer of water of nearly constant temperature until the freezing point is reached. When sea ice begins to form, the salinity of this isothermal layer will start to increase as a result of the haline convection caused by the introduction of dense, highly-saline brine, that is excluded from the ice matrix, to the top of the layer. Since the water undergoes a phase change on freezing, the liquid phase will not change temperature until the entire body of water is frozen, with the exception of the boundary layer at the top where some slight supercooling may occur. Near the freezing point the coefficient of thermal expansion of sea water is very small, and thus any thermally produced buoyancy effects will be very much smaller than haline effects produced by sea ice formation and can be neglected.

We will assume that sea water can be treated as an incompressible fluid with constant properties, except for density as it affects the buoyancy (the Boussinesq approximation). We further assume that the layer of sea water is at the freezing point and remains isothermal during the course of the process. The equation of state is then quite accurately represented by

$$\rho=\rho_0[1+\gamma(S-S_0)], \tag{1}$$

where ρ is the density, γ the salinity coefficient of volume expansion, S the salinity, and the subscript zero indicates the reference state. We will take for a length scale the depth of the fluid layer h, for a time scale h^2/D where D is the kinematic form of the diffusivity of salt in sea water, and for a salinity scale $Fh/(\rho D\gamma)$ where F is the rate of salt flux into the fluid layer. We will assume that the motions in the ocean can be represented to a first approximation by a two-dimensional model in which there are no variations in the horizontal y direction. It is convenient to divide the salinity S into a horizontal mean $\bar{S}(z,t)$ and a fluctuating part $s(x,z,t)$, so that $S=\bar{S}+s$ and $\bar{s}=0$. Under these conditions the continuity equation becomes

$$\frac{\partial u}{\partial x}+\frac{\partial w}{\partial z}=0, \tag{2}$$

and the diffusion equation

$$\frac{\partial \bar{S}}{\partial t}+\frac{\partial s}{\partial t}+u\frac{\partial s}{\partial x}+w\frac{\partial s}{\partial z}+w\frac{\partial \bar{S}}{\partial z}=\left(\frac{\partial^2}{\partial x^2}+\frac{\partial^2}{\partial z^2}\right)s+\frac{\partial^2 \bar{S}}{\partial z^2}. \tag{3}$$

The Navier-Stokes equations can be manipulated to yield

$$\frac{1}{\sigma}\frac{\partial}{\partial t}\left(\frac{\partial^2}{\partial x^2}+\frac{\partial^2}{\partial z^2}\right)w-\frac{1}{\sigma}\frac{\partial}{\partial x}\left(u\frac{\partial}{\partial x}+w\frac{\partial}{\partial z}\right)\left(\frac{\partial u}{\partial z}-\frac{\partial w}{\partial x}\right)=\left(\frac{\partial^2}{\partial x^2}+\frac{\partial^2}{\partial z^2}\right)^2 w-\mathrm{R}\frac{\partial^2 s}{\partial x^2}, \tag{4}$$

where

$$\sigma=\nu/D \tag{5}$$

is the Schmidt number,

$$\mathrm{R}=gFh^4/(D^2\nu\rho) \tag{6}$$

is the Rayleigh number, g the acceleration of gravity, and ν the kinematic viscosity. We have taken z to be vertically downward so that the top surface is at $z=0$ and the bottom at $z=1$.

We will assume that the horizontal boundary surfaces at top and bottom are flat but incapable of supporting tangential stresses; thus,

$$w=\frac{\partial^2 w}{\partial z^2}=0 \quad \text{at} \quad z=0,\ 1. \tag{7}$$

These so-called "free boundary conditions" are not realistic but the errors introduced should be small (Foster, 1968b) and the behavior of the system should be correctly represented, at least qualitatively. It will be assumed that the fluid is infinite in horizontal extent and thus no boundary conditions will be imposed in the horizontal direction. The net salt flux will be taken as a constant value at the top and zero at the bottom;

thus, the boundary conditions for the horizontal mean salinity become

$$\frac{\partial\bar{S}}{\partial z}=-1 \text{ at } z=0, \quad \frac{\partial\bar{S}}{\partial z}=0 \text{ at } z=1. \tag{8}$$

We now assume that the flow is periodic in the horizontal direction and that this periodicity can be represented by a single dimensionless horizontal wavenumber a. In this pseudo two-dimensional model the nonlinear interactions affect only the mean salinity field and the solution of the equations is greatly simplified. This simplification has been called the "mean field approximation," and has been used successfully by Herring (1963) for the investigation of thermal convection. The basic difficulty with this simplification is that it does not provide a mechanism for the selection of the horizontal wavenumber; however, in many examples of hydrodynamic instability, such as thermal convection or Couette flow, maximum growth rate has provided a good criterion for the selection of the horizontal wavenumber. In laboratory experiments on haline convection induced by the freezing of sea water (Foster, 1969) it was found that the disturbance which is largest at onset of convection dominates the subsequent flow, a theoretical assumption (Foster, 1968a) which provided a good prediction of the horizontal wavenumber. We will therefore investigate disturbances with a range of wavenumbers and select the wavenumber of the disturbance which has the largest amplitude at some fixed time just before onset of convection as the wavenumber for the convection that actually develops. Onset of manifest convection in this nonlinear model can be designated as the time when the velocity disturbance starts to significantly interact with the mean salinity field (i.e., when the convective terms, $u\partial s/\partial x$ and $w\partial s/\partial z$, become of the same order of magnitude as the rest of the terms in the diffusion equation).

When the mean field approximation and the free boundary conditions (7) are used, a very efficient means for solving the equations is expansion of the variables in Fourier series. Thus, to satisfy the boundary conditions (7) we let

$$w=\Sigma_n A_n(t)\sin(n\pi z)\cos(ax). \tag{9}$$

Similarly, to satisfy the boundary conditions (8) we let

$$\bar{S}=\Sigma_n B_n(t)\cos(n\pi z)+(3z^2-6z+2)/6+t. \tag{10}$$

We also can let

$$s=\Sigma_n C_n(t)\sin(n\pi z)\cos(ax). \tag{11}$$

Substituting (9) into the continuity equation (2) we can solve for u and obtain

$$u=-\Sigma_n A_n(t)(n\pi/a)\cos(n\pi z)\sin(ax). \tag{12}$$

These expansions for w, $\bar{S}$, s and u are substituted into the diffusion equation (3). If we then multiply (3) by $\sin(r\pi z)\cos(ax)$ and integrate from $x=0$ to $x=2\pi/a$ and from $z=0$ to $z=1$, we obtain

$$C_r'(t)=\Sigma_n A_n(t)[\delta_{nr}-I_{nr}+\Sigma_m B_m(t)J_{nmr}] -C_r(t)(r^2\pi^2+a^2), \tag{13}$$

where

$$I_{nr}=\begin{cases}[4nr/\pi^2(n^2-r^2)^2][(-1)^{n+r}-1], & \text{if } n\neq r,\\ \tfrac{1}{2}, & \text{if } n=r,\end{cases}$$

and

$$J_{nmr}=\left[\frac{1}{n+m+r}-\frac{1}{n+m-r}-\frac{1}{n-m+r}+\frac{1}{n-m-r}\right]\times\left[\frac{(-1)^{n+m+r}-1}{\pi}\right].$$

If we multiply (3) by $\cos(r\pi z)$ and integrate from $x=0$ to $x=2\pi/a$ and from $z=0$ to $z=1$, we obtain

$$B_r'(t)=-\Sigma_n\Sigma_m rn\pi^2[A_n(t)C_m(t)+A_m(t)C_n(t)]K_{nmr} -r^2\pi^2 B_r(t), \tag{14}$$

where

$$K_{nmr}=\left[-\frac{1}{n+m+r}-\frac{1}{n+m-r}+\frac{1}{n-m+r}+\frac{1}{n-m-r}\right]\times\left[\frac{(-1)^{n+m+r}-1}{8\pi}\right].$$

We also substitute these expansions into the momentum equation (4), multiply by $\sin(r\pi z)\cos(ax)$, and integrate from $x=0$ to $x=2\pi/a$ and from $z=0$ to $z=1$; thus

$$A_r'(t)=-\sigma A_r(t)(r^2\pi^2+a^2)+\sigma \mathrm{R}a^2C_r(t)/(r^2\pi^2+a^2). \tag{15}$$

The expansions are then truncated to N terms each. Consequently we have $3N$ coupled ordinary differential equations for the Fourier coefficients $A_n(t)$, $B_n(t)$ and $C_n(t)$ which can be solved numerically as an initial value problem using the Runge-Kutta-Gill fourth-order method (Romanelli, 1960).

3. Results

The behavior of the theoretical model was investigated by starting with an isohaline fluid, represented by setting the $B_n(0)=2/(n^2\pi^2)$, and introducing a small "white noise" velocity disturbance, represented by setting the $A_n(0)=10^{-1}$. The initial salinity disturbance was assumed to be negligible and therefore the $C_n(0)=0$. The subsequent development of the system was followed by calculating the mean salinity and the vertical velocity profiles at regular intervals of time. The growth of the disturbances was monitored by calculating an rms average of the vertical velocity

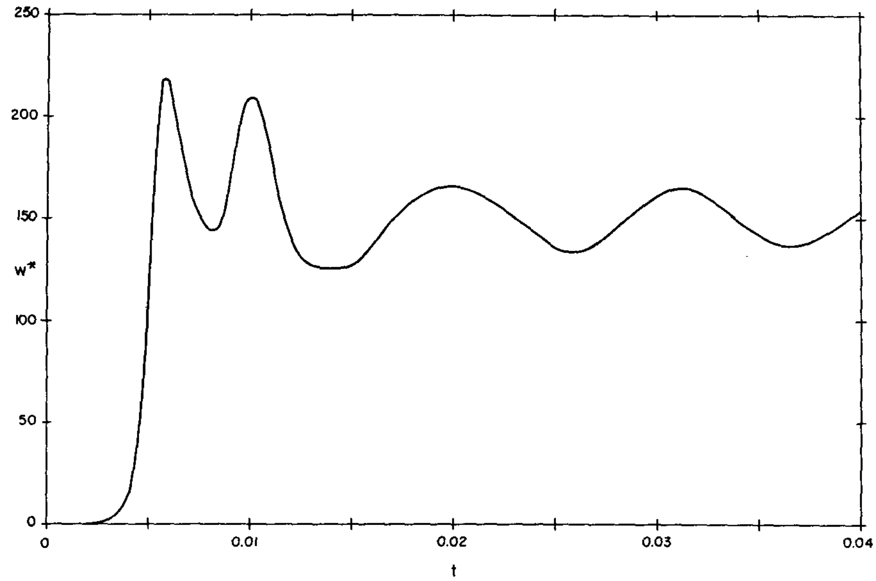

FIG. 3. Development of the rms vertical velocity for $R=10^7$, $\sigma=10$ at optimum wavenumber, $a=13$.

defined as

$$w^*=\left(\int_0^1 w^2dz\right)^{\frac{1}{2}}, \tag{16}$$

where w^* is similar to $\bar{w}$ used in the linear theory (Foster, 1968a), but is not normalized with respect to the initial disturbance. A CDC 3600 computer was used in all calculations. Computer memory limited the number of terms in the Fourier series that could be handled economically to 27 and thus accurate calculations could only be carried out for Rayleigh numbers up to about 10^8.

In the ocean the primary diffusive transport mechanism is turbulent stirring. Thus, the present analysis can be applied to the oceanic convection if the coefficients of viscosity and salt diffusion are considered to be eddy exchange coefficients. On theoretical grounds one would expect that the transport of momentum and salt by turbulence would be of the same order of magnitude; however, observations of the time and space variations of salinity in the ocean have shown that the transport of salt is probably slower then the transport of momentum. Defant (1961) has estimated that the effective Schmidt number for turbulent stirring in the ocean is of the order of 5–20. We will, therefore, investigate our system for Schmidt numbers of 1, 10 and 20 so as to cover the entire probable range for the ocean.

Fig. 3 shows the development of w^* for a Rayleigh number of 10^7 and effective Schmidt number of 10 from the quiescent initial state to a state of fully developed convection. The oscillations in the intermediate stages of development should be noted. A number of investigators (e.g., Townsend, 1959) have observed oscillatory behavior in convective systems at high Rayleigh numbers. In the case of an infinite Schmidt number fluid, which is nearly realized for sea water with molecular coefficients, an analysis similar to the one presented here (Foster, 1971) showed that the system did not settle down to a steady state but continued to exhibit oscillations for Rayleigh numbers $\gtrsim 10^7$. The onset of truly intermittent convection is associated with the instability of the salinity boundary layer at the top of the fluid. For decreasing values of the Schmidt number the critical horizontal wavenumber a_c increases, and thus the horizontal spacing of the convection cells decreases. Therefore, for Schmidt numbers in the range 1–20 the salinity boundary layer will have a smaller lateral extent in each cell and have less of a tendency to flow off impulsively than in the case of a fluid with infinite Schmidt number. Thus, fully intermittent convection probably requires larger Rayleigh numbers for Schmidt numbers between 1 and 20 than could be investigated using the present technique. Extrapolation of the results of calculations for Rayleigh numbers less than 10^8 to larger numbers, therefore, entails some uncertainty, but it is believed that the cell sizes and velocities predicted in this way would not be greatly in error, certainly by less than an order of magnitude. Depending upon the depth of the isothermal layer and the freezing rate, the Rayleigh number in the ocean ranges from about 10^5 to 10^{14}. The present analysis thus covers the lower part of the range directly and the higher part indirectly by extrapolation.

Fig. 4 shows the mean salinity profile for $R=10^7$ and $\sigma=10$ at $t=10^{-2}$, which is typical of the oscillatory regime, and at $t=4\times10^{-2}$, which is typical of a state of fully-developed convection. At $t=10^{-2}$ a dense, highly saline blob has just broken away from the top boundary layer and can be seen about halfway down, This type of salinity profile is similar to those found for fully intermittent convection (see Fig. 2, Foster, 1971) and is to be expected for high Rayleigh numbers at any time. At $t=4\times10^{-2}$ the salinity profile is characterized by a quasi-steady state with a thin, high salinity boundary layer at top and the bulk of the fluid nearly isohaline. This type of profile is to be expected at low Rayleigh numbers, less than about 10^9.

Fig. 5 shows the variation of horizontal wavenumber for optimum growth as a function of Rayleigh number for Schmidt numbers of 1, 10, 20 and ∞. It is seen that, as the Rayleigh number increases, the horizontal wavenumber tends to increase as $R^{\frac{1}{4}}$. Since the Rayleigh number is a function of the depth of the fluid layer to the fourth power and the wavenumber is made dimensionless by the depth, the $\frac{1}{4}$ power dependence shows that for large R the dimensional wavenumber and, thus, cell spacing become independent of depth. The same is true for the vertical velocity which shows a $R^{\frac{1}{4}}$ dependence for large R. The time that is required for manifest convection to set in, shows a $-\frac{1}{2}$ power dependence on Rayleigh number. Since time is made dimensionless by a factor containing depth to the inverse square power, the $R^{-\frac{1}{2}}$ dependence shows that the dimensional critical time is also independent of depth at large R.

Since it is apparent that for large Rayleigh numbers, greater than about 10^7, the convective system does not depend upon the depth of the fluid layer, it is useful to derive expressions for the dimensional horizontal wavelength λ, the dimensional maximum vertical velocity in the quasi-steady state, w_{max}, and the dimensional time required for manifest convection to set in, t_c, which show this depth independence explicitly. Thus

$$\lambda=C_1(D^2\nu\rho/gF)^{\frac{1}{4}}, \tag{17}$$

$$w_{max}=C_2(D^2gF/\nu\rho)^{\frac{1}{4}}, \tag{18}$$

$$t_c=C_3(\nu\rho/gF)^{\frac{1}{2}}. \tag{19}$$

The constants C_1, C_2 and C_3 depend upon the Schmidt number as shown in the following table:

σ	C_1	C_2	C_3
1	24	4.7	28
10	27	5.2	17
20	31	6.1	15
∞	48	6.3	14

These formulae should allow *estimation* of the parameters of haline convection in the ocean. It should be cautioned that the approximations used in deriving these formulae may have introduced inaccuracies in the numerical constants. The maximum vertical velocities [(18)] and times required for manifest convection to set in [(19)] should be viewed as accurate only in an order-of-magnitude sense. The horizontal spacing of convection cells calculated using (17) is most likely more accurate, the error probably being less than a factor of 2.

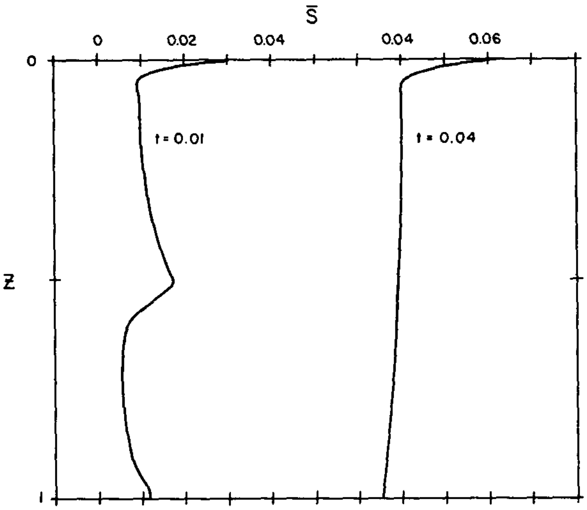

FIG. 4. Mean salinity profiles for $R=10^7$, $\sigma=10$, $a=13$ in the oscillatory regime, $t=0.01$, and in the quasi-steady state, $t=0.04$.

4. Application to the ocean

The foregoing analysis can be directly applied to the ocean only where there is an isothermal layer that is initially isohaline. These conditions are very nearly met in the uppermost layer of the surface water in the Weddell Sea in winter. Fig. 1 shows that the isothermal layer is generally 100 m thick and that this layer is also usually isohaline in the top 50–100 m. The theory

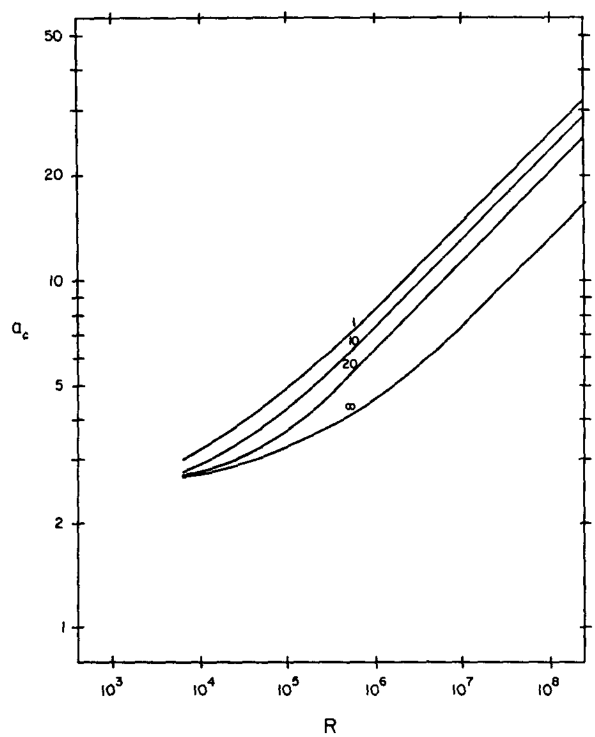

FIG. 5. Variation of horizontal wavenumber as a function of Rayleigh number for various Schmidt numbers.

can easily be extended to cases where the initial salinity profile is not isohaline by changing the initial conditions, i.e., by starting with different $B_n(0)$. The theory for such cases would not be general and formulae, such as (17)–(19), would have to be derived for each unique set of initial conditions. The inclusion of cases where the initial temperature profile is not isothermal would involve a major revision to the theory, as then the equation of state would involve two variables.

For a rough approximation let us assume that the conditions observed in the polynya of Fig. 2 are typical and that an average of 1 cm of ice forms in 1 hr. If the sea ice has a salinity 30‰ less than the sea water from which it forms, then for each cubic centimeter of sea ice formed 0.027 gm salt will be introduced to the water layer just beneath the ice. For the above average ice growth rate the salt flux would thus be $F=7\times10^{-6}$ gm cm^{-2} sec^{-1}. Munk (1966), in agreement with other investigators, estimated that the eddy diffusivity for the deep ocean is on the order of 1 cm^2 sec^{-1}. Since the ice cover of polar regions would restrict surface waves, the eddy exchange coefficients under the ice sheet might be similar to the deep ocean. So for lack of any measurements let us take the value 1 cm^2 sec^{-1} for both the viscosity and diffusivity; the Schmidt number is thus unity. The horizontal cell spacing under such conditions calculated using (17) is about 80 cm; the maximum vertical velocity (18) is about 1.4 cm sec^{-1}; and the time needed for the onset of manifest convection (19) is about 5 min. Thus, since the horizontal scale of the convective flow is less than 1 m, we would expect that the conditions of horizontal homogeneity we assumed would be attained for leads wider than about 10 m. The present analysis should, therefore, be applicable to most leads and polynyas.

In a previous theoretical paper on haline convection (Foster, 1968a) it was speculated that a cascade, or hierarchy, of larger and larger convection cells might form due to successive instabilities. A tendency for haline convection to exhibit a secondary instability was observed during the course of laboratory experiments (Foster, 1969). Previously, we could only guess as to how the hierarchy of convective eddies developed since only the case for infinite Schmidt number was treated and velocities could not be determined as the theory was linear. We can now use the present, more general, nonlinear theory to make a better estimation of the possible development of convective eddies. To begin let us assume that a smooth ice sheet starts to form on the sea surface as is regularly observed in open leads and polynyas which are not greatly disturbed by surface waves. The molecular coefficients of viscosity and diffusivity are then appropriate. For sea water of 34‰ salinity at the freezing point the kinematic viscosity is about 2×10^{-2} cm^2 sec^{-1}, and the diffusivity about 7×10^{-6} cm^2 sec^{-1}; this gives a Schmidt number of about 3×10^3 which is for the present theory effectively infinite. If we use the same typical freezing rate for a polynya as before, the salt flux is 7×10^{-6} gm cm^{-2} sec^{-1}; the horizontal spacing of cells then becomes about 0.2 cm, and the maximum vertical velocity about 0.01 cm sec^{-1}. This convection would take about 20 sec to develop.

The laboratory experiments showed that haline convection takes the form of long streamers or filaments, which could be traced for more than 10 cm. In the ocean, the limitation to the depth to which these streamers could penetrate in a coherent manner is determined by their diameter and the salt diffusivity. The time required for the salt in the center of the streamer to diffuse away significantly is on the order $\lambda^2/(4D)$. Thus, for the above example, the streamers would be coherent to a depth on the order of 10 cm. We would expect that the convection would cease to transport salt in a coherent cell-like structure to depths much greater than this. The overall transport would then again become diffusive but with turbulence providing random motion analogous to irregular molecular motion. If we assume that the depth that the streamers are coherent is the analog of the molecular mean free path, a very rough estimate of the eddy exchange coefficients is the product of this depth and the vertical velocity of the streamers. Thus, for the example being considered, we obtain eddy coefficients on the order of 0.2 cm^2 sec^{-1}. Since the transport is now diffusive, penetration would proceed like $(At)^{\frac{1}{2}}$ where A is the eddy coefficient. Thus, a new unstable salinity boundary layer could be produced, though considerably thicker than the one due to molecular diffusion. Using the constants appropriate for a Schmidt number of unity in Eqs. (17)–(19) we find that the secondary convection would have a horizontal cell spacing of about 20 cm, a maximum vertical velocity of about 0.9 cm sec^{-1}, and would take about 2 min to develop after the primary convection became fully developed ($\sim$15 min). The difference in effectiveness as a transport mechanism between organized convection and turbulent diffusion can be seen from the above example. Turbulent diffusion with an eddy coefficient of 0.2 cm^2 sec^{-1} would require about $d^2/A=5\times10^4$ sec to penetrate a distance $d=1$ m; while convection with a vertical velocity of 0.9 cm sec^{-1} would require $d/w\approx10^2$ sec to penetrate the same distance, or more than two orders of magnitude faster.

It seems very difficult to even speculate as to what might be the next stage in the convective process. The depth to which organized convection might penetrate before turbulent diffusion would dissipate the streamers would now be on the order of 6 m. The secondary convection should generate eddy coefficients on the order of 500 cm^2 sec^{-1}. The tertiary convection would then have a horizontal cell spacing of about 90 m, a maximum vertical velocity of about 6 cm sec^{-1} and would take about 2 hr to develop. This tertiary convection could penetrate over 2 km before it would be dissipated by diffusion. However, it is not at all clear that the eddy coefficient would still be 0.2 $cm^2\ sec^{-1}$ in the fluid through which the streamers are falling except in the top layer. Thus, it also seems possible that the secondary convection might not take the form of streamers, such as those that have been observed in the primary convection, where the Schmidt number is effectively infinite, but rather the convection might occur in the form of intermittent blobs of dense, saline fluid breaking away from the diffusive boundary layer under the ice sheet. This seems to be the form that turbulent convection takes in the atmosphere and is usually given the name "thermals." These dense saline blobs, a kind of inverted thermals, might penetrate to the bottom of the isohaline, isothermal layer under a growing ice sheet. In this case a higher order instability might not develop. Recent studies, however, of large-scale convection in the Mediterranean (Stommel *et al.*, 1971) seem to indicate that the convection is intermittent and takes place through a hierarchy of scales. It seems obvious that further observations are necessary in order to determine the form that the process of haline convection takes in the ocean.

We can conclude that in polynyas and in most leads the haline convection induced by the freezing of sea water will take place by an instability of the salinity boundary layer with horizontal scales generally less than a meter. If a hierarchy of convection scales develops, horizontal scales larger than the width of most leads may occur; in this case the horizontal inhomogeneity at the ice boundary may become important. In any case, haline convection would appear to be an effective vertical transport mechanism and is probably an important precursor to Antarctic Bottom Water formation in the Weddell Sea.

Acknowledgments. This work was supported by the Office of Naval Research under Contract N00014-69-A-0200-6009.

REFERENCES

Badgley, F. I., 1966: Heat budget at the surface of the Arctic Ocean. *Proc. Symp. Arctic Heat Budget and Atmospheric Circulation,* RAND Corp. Memo. RM-5233-NSF, 267–277.

Brennecke, W., 1921: Die ozeanographischen Arbeiten der deutschen Antarktischen Expedition 1911–1912. *Arch. Deut. Seewarte,* **39**, No. 1, 215 pp.

Coachman, L. K., 1966: Production of supercooled water during sea ice formation. *Proc. Symp. Arctic Heat Budget and Atmospheric Circulation,* RAND Corp. Memo. RM-5233-NSF, 497–529.

Deacon, G. E. R., 1937: The hydrology of the Southern Ocean. *Discovery Rept.*, **15**, 124 pp.

Defant, A., 1961: *Physical Oceanography*, Vol. I. New York, Pergamon, p. 103.

Fletcher, J. O., 1969: Ice extent on the Southern Ocean and its relation to world climate. RAND Corp. Memo. RM-5793-NSF, 108 pp.

Foster, T. D., 1968a: Haline convection induced by the freezing of sea water. *J. Geophys. Res.*, **73**, 1933–1938.

——, 1968b: Effect of boundary conditions on the onset of convection. *Phys. Fluids*, **11**, 1257–1262.

——, 1969: Experiments on haline convection induced by the freezing of sea water. *J. Geophys. Res.*, **74**, 6967–6974.

——, 1971: Intermittent convection. *Geophys. Fluid Dyn.*, **2**, 201–217.

——, 1972: An analysis of the cabbeling instability in sea water. *J. Phys. Oceanogr.* **2**, 294–301.

Herring, J. R., 1963: Investigation of problems in thermal convection. *J. Atmos. Sci.*, **20**, 325–338.

Mosby, H., 1934: The waters of the Atlantic Antarctic Ocean. *Det. Norske Viden. Akad., Sci Res., Norwegian Antarctic Exped.*, 1927–1928, **1**, No. 11, 117 pp.

Munk, W. H., 1966: Abyssal recipes. *Deep Sea Res.*, **13**, 707–730.

Romanelli, M. J., 1960: Runge-Kutta methods for the solution of ordinary differential equations. *Mathematical Methods for Digital Computers*, New York, Wiley, 110–120.

Stommel, H., A. Voorhis and D. Webb, 1971: Submarine clouds in the deep ocean. *Amer. Scientist*, **59**, 716–722.

Townsend, A. A., 1959: Temperature fluctuations over a heated horizontal surface. *J. Fluid Mech.*, **5**, 209–241.

Witte, E., 1902: *Zur Theorie der Stromkabbelung.* Gaea, Köln, 484–487.

Wittmann, W. I., and J. J. Schule, 1966: Comments on the mass budget of arctic pack ice. *Proc. Symp. Arctic Heat Budget and Atmospheric Circulation*, RAND Corp. Memo. RM-5233-NSF, 217–246.

Wüst, G., 1938: Bodentemperatur und Bodenstrom in der Atlantischen, Indischen und Pazifischen Tiefsee. *Beitr. Geophys.*, **54**, 1–8.

Zubov, N. N., 1943: *Arctic Ice.* English translation edited by U. S. Navy Electronics Laboratory, 491 pp.